



Cite this: *Dalton Trans.*, 2014, **43**, 16173

Received 18th July 2014,
Accepted 9th September 2014

DOI: 10.1039/c4dt02176b

www.rsc.org/dalton

Chemical “top-down” synthesis of amphiphilic superparamagnetic Fe₃O₄ nanobelts from exfoliated FeOCl layers†

Xiao Wei, Juan Su, Xin-Hao Li* and Jie-Sheng Chen

A novel chemical “top-down” method has been employed to prepare tiny Fe₃O₄ nanobelts. Uniform Fe₃O₄ nanobelts were obtained by solvothermal reduction of exfoliated FeOCl layers with the assistance of high polar solvents and a PEO–PPO–PEO stabilizer. We also studied the superparamagnetic properties of Fe₃O₄ nanobelts, which exhibit a magnetic saturation value as high as ~53 emu g⁻¹ at room temperature and a magnetic anisotropy constant up to 6.6 × 10⁴ erg cm⁻³. Furthermore the as-obtained product, which is amphiphilic and exhibits excellent dispersibility and redispersibility in most of the common solvents, could be readily used in various realms of biomedicine and biotechnology.

Introduction

One-dimensional (1D) nanostructures, including nanowires, nanorods and nanobelts, have drawn much attention because they show great promise in the manufacture of nanoelectronic devices, sensors and field emission devices, as well as in spintronic and medical applications.^{1–10} Among the one-dimensional nanostructures, magnetic nanorods, nanobelts and nanowires with an elongated structure exhibit magnetic anisotropies. Most of the applications of magnetic materials in technology and industry nowadays are probably determined by the magnetic anisotropy, that is, the dependence of magnetic properties on a preferred direction in response to thermal or magnetic stimuli. Therefore, the one-dimensional magnetic nanostructures are potentially applicable as hard magnetic materials and ferrofluids in magnetic recording, magnetic hyperthermia and related realms.^{11–19} However, the approaches for the synthesis of uniform one-dimensional magnetic nanostructures, especially *via* solution-phase approaches, are really limited at the moment.

Besides one-dimensional nanostructures, the surface modification is another aspect that should be considered for their practical applications, especially in the realms of drug delivery and magnetic resonance imaging (MRI). Consider the success in fabricating magnetic nanoparticles in oil phase, much efforts have been devoted to replacing the hydrophobic ligands of as-obtained magnetic nanoparticles with polar ones to make them hydrophilic for biological use. As an alternative, amphiphilic magnetic nanoparticles that are dispersible in both polar and nonpolar solvents should be ideal candidates for these applications. Although amphiphilic magnetic spheres with a size larger than 100 nm have been prepared in our previous work,²⁰ the large size of these materials limited their applications in *in situ* hyperthermia. This is because only tiny nanoparticles smaller than 50 nm can penetrate through the cell membrane. Developing an efficient method for fabricating fine nanostructures with an amphiphilic surface is thus highly alluring but remains a great challenge.

A variety of techniques have been exploited to prepare magnetic nanostructured particles in the past.^{21–24} Especially the colloidal chemical synthesis^{14,25–28} of nanoparticles has been intensively pursued because both the size and the shape of the nanoparticles may be finely controlled through this synthetic technique. Generally, for synthesis of nanoparticles, the solution colloidal chemical approaches can be designated “bottom-up” methods. “Top-down” methods are mostly conventional physical techniques, through which the preparation of uniform nanoparticles with controlled sizes and shapes from bulk phase is hard to achieve. However, the advantage of “top-down” methods for synthesizing anisotropic 1D or 2D nanostructures is obvious, whilst “bottom-up” methods usually tend to boost the formation of nanoparticles with low structural anisotropy.

Herein, we show the proof-of-principle application of the “top-down” method for preparing uniform nanobelts. We applied a novel chemical “top-down” method combined with a solvothermal process to transfer exfoliated FeOCl layers to nearly uniform superparamagnetic Fe₃O₄ nanobelts. The Fe₃O₄ nanobelts exhibited a magnetic saturation value as high

School of Chemistry and Chemical Technology, Shanghai Jiao Tong University, Shanghai 200240, P. R. China. E-mail: xinhaoli@sjtu.edu.cn;

Fax: +86 021 5474 1297

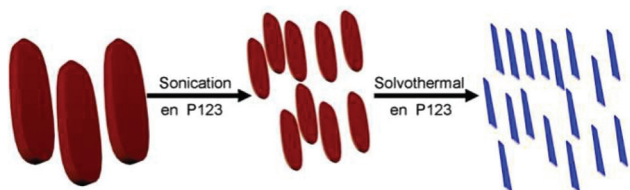
† Electronic supplementary information (ESI) available: SEM image of FeOCl, TEM image of Fe₃O₄ aggregates obtained without an exfoliating process and magnetic hysteresis loops of Fe₃O₄ nanobelts. See DOI: 10.1039/c4dt02176b

as $\sim 53 \text{ emu g}^{-1}$ at room temperature and a magnetic anisotropy constant of up to $6.6 \times 10^4 \text{ erg cm}^{-3}$. Moreover, the excellent dispersibility of the tiny Fe_3O_4 nanobelts in both polar and non-polar solvents was also investigated in this work.

Experimental

FeOCl was selected as a possible precursor for the synthesis of nanobelts due to its layered structure and unique composition containing Fe and O species simultaneously. Inorganic layered materials, such as layered double hydroxides (LDH) and FeOCl , have been widely used in catalysis, adsorption, nano-composite formation, and drug delivery.^{29–32} Recently, there were several reports on the preparation of stable suspensions of LDHs,^{29,33,34} and nanoparticles have also been obtained using the layered materials as templates or scaffolds.^{35,36} However, further transferring these layered materials into even smaller nanostructures *via* chemical redox reactions has never been attempted till now.

In our experiment, the layered millimeter or micrometer sized bulk FeOCl (Fig. S1†) was firstly prepared by following the procedures described elsewhere.³⁷ Typically, a mixture of 12.986 g of FeCl_3 and 9.582 g of Fe_2O_3 was sealed in a glass tube under vacuum and heated at 385 °C for a week. The as-obtained FeOCl product was washed thoroughly with acetone and finally dried under vacuum. Further exfoliation of FeOCl was conducted *via* sonication for 300 cycles of 5 s on and 5 s off pulses with an output power of 400 W in ethylenediamine (en) and *block*-copolymer poly(ethylene glycol)-*block*-poly(propylene glycol)-*block*-poly(ethylene glycol) (PEO-PPO-PEO or P123). The as-formed stable colloidal suspension was then sealed in a 50 mL PTFE-lined stainless steel autoclave and heated at 140 °C for 12 h under static conditions followed by slow cooling to room temperature. The resulting product was thoroughly washed with absolute ethanol and a mixture of ethanol and deionized water to remove all residual reagents, and separated through centrifugation. The whole formation mechanism of Fe_3O_4 nanobelts is summarized in Scheme 1. In the reaction process, Fe^{2+} cations were formed *via* reduction of a fraction of Fe^{3+} ions by the ethylenediamine, then smaller Fe_3O_4 nanobelts were formed. Therefore, our synthetic approach can be ascribed to the chemical “top-down” method.



Scheme 1 Synthetic pathways for the synthesis of Fe_3O_4 nanobelts (blue) *via* a two-step method: (1) exfoliating FeOCl solid (red) into FeOCl layers with the presence of en and P123 followed by (2) solvothermal reduction of exfoliated FeOCl layers into Fe_3O_4 nanobelts (blue).

It is obvious that the belt structure of the final Fe_3O_4 nanobelts was mainly replicated from the layered precursor, exfoliated FeOCl nanosheets. P123 stabilized the as-formed nanosheets or nanobelts during the whole synthetic process.

Results and discussion

Fig. 1 shows the transmission electron microscopy (TEM) images of Fe_3O_4 nanobelts. It is seen that the width ($\sim 17 \text{ nm}$, Fig. 1A) and the thickness (1–4 nm, Fig. 1C) of the nanobelts are nearly uniform while the length of the nanobelts is polydisperse, ranging from 30 to 200 nm. The selected-area electron diffraction (SAED) pattern as shown in Fig. 1 further confirms the formation of crystalline Fe_3O_4 nanobelts. All these TEM results suggested the success of our chemical “top-down” method for transferring bulk FeOCl solid into tiny nanobelts. Further extending our principle to the synthesis of metal oxide nanobelts or nanosheets is still in progress by solvothermal reduction of exfoliated small sheets of specific LDHs.

It is worth noting that the process of exfoliating the layered FeOCl is of key importance for the synthesis of nearly uniform Fe_3O_4 nanobelts. The intense sonication of FeOCl solid before the solvothermal reaction is also highly required to get a stable FeOCl colloidal solution and finally Fe_3O_4 nanobelts; otherwise, we probably could get large micrometer sized aggregates rather than Fe_3O_4 nanobelts (Fig. S3†). Moreover, the tempera-

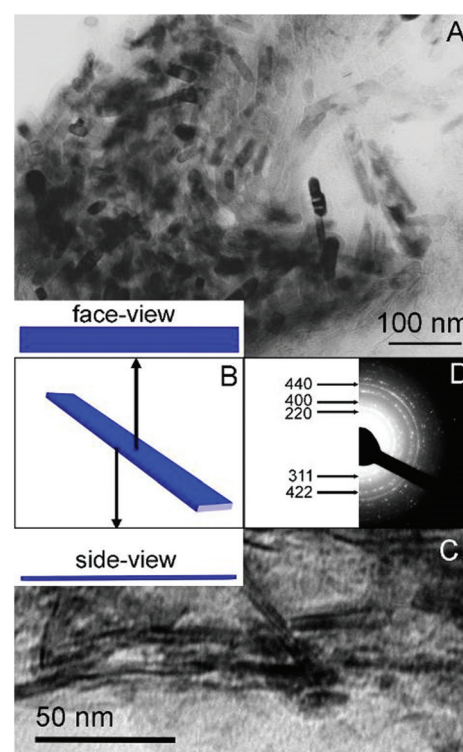


Fig. 1 Face-view (A) and side-view (C) TEM images, simulated models (B) and SAED pattern (D) of typical Fe_3O_4 nanobelts.

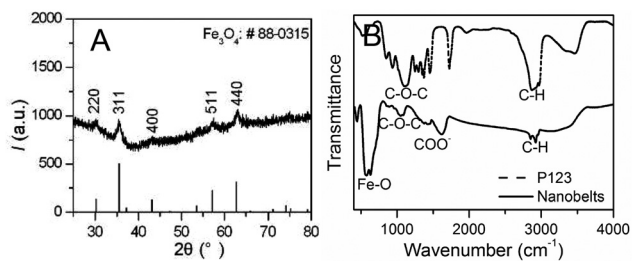


Fig. 2 XRD pattern (A) of Fe_3O_4 nanobelts, and FTIR spectra (B) of Fe_3O_4 nanobelts and P123. Bars in A: JCPDS No. 88-0315.

ture, at which the precursors were solvothermally treated, is another key parameter for the preparation of nearly uniform Fe_3O_4 nanobelts. Too high a temperature (for example, $>180^\circ\text{C}$) usually gives rise to the formation of irregular particles or aggregates due to the vigorous reaction process, while too low a temperature (for example, $<120^\circ\text{C}$) might result in a longer reaction time or the formation of impurity ($\alpha\text{-Fe}_2\text{O}_3$). Under optimized conditions (140°C for 12 h), pure Fe_3O_4 nanobelts were obtained. The powder X-ray diffraction (XRD) pattern of Fe_3O_4 nanobelts (Fig. 2A) indicates that the FeOCl is completely converted to Fe_3O_4 . The as-obtained Fe_3O_4 nanobelts are pure-phase ferrites with a cubic structure. The presence of PEO-PPO-PEO in the final product is proved by infrared (IR) spectroscopy. As shown in Fig. 2B, the typical stretching vibrations of C-O-C and C-H appear in the IR spectrum of the Fe_3O_4 nanobelts even after thorough washing with excess amount of ethanol and water. A strong Fe-O peak at 590 cm^{-1} was also observed. Two new peaks at 1407 and 1579 cm^{-1} suggested the formation of COO- groups after the solvothermal reactions. This is to say that a strong interaction between the Fe_3O_4 nanobelt and the organic stabilizer could be expected *via* chemical bonds. All these results indicated that the as-obtained Fe_3O_4 nanobelts are hybrids of Fe_3O_4 and P123.

The presence of P123 on the surface of Fe_3O_4 nanobelts could not only keep them from aggregation, but also afford them an amphiphilic surface. Unlike common nanoparticles, which are either hydrophilic or hydrophobic, the products can be well dispersed in most of the common solvents. For instance, the as-synthesized powder of the Fe_3O_4 nanobelts can be well dispersed in polar and non-polar solvents (Fig. 3A), and form stable colloids. Under optimal conditions, the colloidal solution of the Fe_3O_4 nanobelts in ethanol remains stable for more than four months. More importantly, all these colloidal dispersions are transparent (Fig. 3B) due to the small size of the Fe_3O_4 nanobelts, benefitting for their potential applications in MRI or biomedicine.

The Fe_3O_4 nanobelts remain in the polar solvent or in the non-polar solvent (represented by water and hexane, respectively, as shown in Fig. 3C left), in which they are originally dispersed, without shaking or sonication. This phenomenon demonstrates the amphiphilic nature of the Fe_3O_4 nanobelts. It is believed that the amphiphilic behaviour of the Fe_3O_4

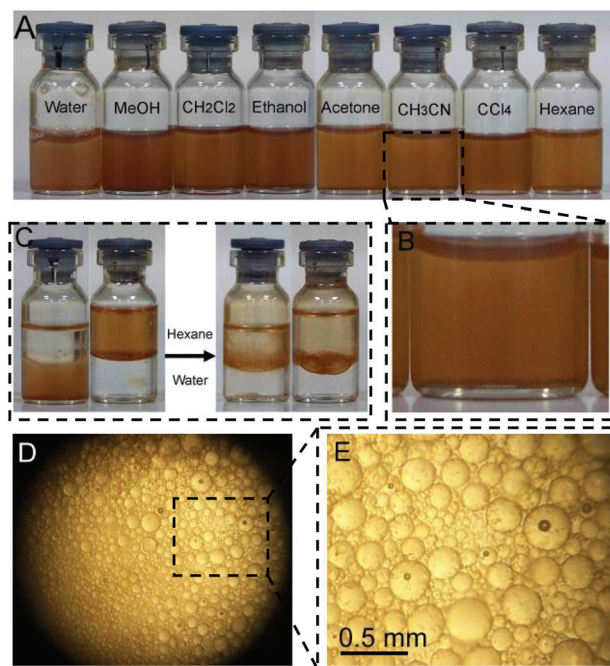


Fig. 3 (A) Suspensions of Fe_3O_4 nanobelts various solvents; (B) amplified image of the transparent dispersion of Fe_3O_4 nanobelts in acetonitrile; (C) left: amphiphilic Fe_3O_4 nanobelts originally dispersed in water or hexane to which hexane or water was added, right: the thin film formed at the water-hexane interface; (D) oil (hexane) in water emulsion stabilized by Fe_3O_4 nanobelts; (E) amplified images of the capsules in the as-formed emulsion with a size ranged from 20 to 450 μm .

nanobelts originates from the PEO-PPO-PEO block copolymer. Gentle shaking or sonication easily moves the amphiphilic Fe_3O_4 nanobelts to the water-hexane interface (Fig. 3C right), and a black/brown thin film forms at the interface and expands upwards along the wall of the glass bottle. As a result, amphiphilic Fe_3O_4 nanobelts can be used to stabilize micro-emulsion (Fig. 3D). Through rigorous shaking, the amphiphilic Fe_3O_4 nanobelts can stabilize the oil-in-water emulsion or reverse emulsion to form hollow capsules as shown in Fig. 3E. These as-obtained capsules with superparamagnetic properties and excellent dispersibility in various common solvents could be good candidates for drug delivery, controlled manipulation of liquid droplets and micro-detection/reaction.²⁹

The magnetic properties of the products were investigated using a superconducting quantum interference device (SQUID) magnetometer. Fig. 4A shows the temperature dependence of field-cooled (FC) and zero-field-cooled (ZFC) magnetization measured with an applied field of 1000 Oe from 300 K to 4 K. On cooling, the zero-field-cooled magnetization begins to drop and deviates from the field-cooled magnetization at 65 K, the blocking temperature (T_B) of the as-obtained Fe_3O_4 nanobelts. Typical hysteresis loops have also been observed for Fe_3O_4 nanobelts at 4 K and 300 K (Fig. 4B). It is seen that the Fe_3O_4 nanobelts are ferromagnetic at 4 K but nearly superparamagnetic at 300 K, consistent with the small size of the Fe_3O_4 nanobelts.^{38,39} At 4 K, the coercive forces (H_c) and the rema-

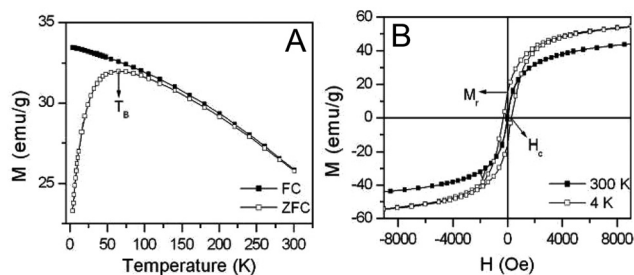


Fig. 4 (A) Temperature dependence of magnetization curves and (B) hysteresis loops of Fe_3O_4 nanobelts.

nence values (M_r) are 287.2 Oe and 15.6 emu g^{-1} , respectively, while the coercivity and remanence values are not obvious at 300 K (Fig. 4B and S4[†]). The magnetic saturation value at 300 K is as high as 53 emu g^{-1} .

As the magnetic anisotropy energy of the nanoparticles deposited on certain surfaces can be tuned by the modification of the size, shape and coupling with the substrate, the synthesis of magnetic nanoparticles with uniform size and controlled shape is tremendously attractive for basic investigations as well as for miniaturized data storage applications. For nanometer-sized magnetite, shape magnetic anisotropy, dependent on the shape anisotropy and the saturation magnetization, is believed to be the dominant form of magnetic anisotropy. Due to the high magnetic saturation value (53 emu g^{-1} at 300 K) and the elongated shape, the as-obtained Fe_3O_4 nanobelts exhibit higher anisotropy. The anisotropy constant (K) of superparamagnetic nanoparticles can be calculated from the T_B using the equation: $K = 25k_B T_B / V$, where k_B is Boltzmann's constant and V is the volume of a single nanoparticle.⁴⁰ For a Fe_3O_4 nanobelt with a length of 100 nm, the calculated magnetic anisotropy constant is as high as $6.6 \times 10^4 \text{ erg cm}^{-3}$. Such a value was much higher than that ($5.2 \times 10^3 \text{ erg cm}^{-3}$) of spherical Fe_3O_4 particles (mean size: 300 nm) obtained *via* a similar protocol.²⁰

Conclusions

We have successfully prepared amphiphilic superparamagnetic Fe_3O_4 nanobelts *via* a novel chemical “top-down” method. This synthetic approach, using the exfoliated layered material FeOCl as a precursor, is facile and easy to scale up for large-quantity application. The as-obtained product, which exhibits nearly uniform width, superparamagnetic properties, obvious magnetic anisotropy and excellent dispersibility and redispersibility in most of the common solvents, could be readily used in various fields such as biomedicine and nanoelectronics.

Acknowledgements

This work was financially supported by the National Basic Research Program of China (2013CB934102, 2011CB808703) and the National Natural Science Foundation of China (21331004, 21301116).

Notes and references

- 1 S. Iijima, *Nature*, 1991, **354**, 56.
- 2 J. T. Hu, T. W. Odom and C. M. Lieber, *Acc. Chem. Res.*, 1999, **32**, 435.
- 3 Y. Xia, P. Yang, Y. Sun, Y. Wu, B. Mayers, B. Gates, Y. Yin, F. Kim and H. Yan, *Adv. Mater.*, 2003, **15**, 353.
- 4 J. Zimmerman, R. Parameswaran and B. Z. Tian, *Biomater. Sci.*, 2014, **2**, 619.
- 5 Z. L. Wang, *ACS Nano*, 2008, **2**, 1987.
- 6 F. S. Kim, G. Ren and S. A. Jenekhe, *Chem. Mater.*, 2010, **23**, 682.
- 7 T. Zhai, L. Li, X. Wang, X. Fang, Y. Bando and D. Golberg, *Adv. Funct. Mater.*, 2010, **20**, 4233.
- 8 T. Zhai, L. Li, Y. Ma, M. Liao, X. Wang, X. Fang, J. Yao, Y. Bando and D. Golberg, *Chem. Soc. Rev.*, 2011, **40**, 2986.
- 9 N. W. S. Kam, Z. Liu and H. Dai, *J. Am. Chem. Soc.*, 2005, **127**, 12492.
- 10 Y. Lei, Q. Liao, H. Fu and J. Yao, *J. Am. Chem. Soc.*, 2010, **132**, 1742.
- 11 A. Fert and L. Piroux, *J. Magn. Magn. Mater.*, 1999, **200**, 338.
- 12 J. Dorantes-Dávila and G. M. Pastor, *Phys. Rev. Lett.*, 1998, **81**, 208.
- 13 P. Gambardella, A. Dallmeyer, K. Maiti, M. C. Malagoli, W. Eberhardt, K. Kern and C. Carbone, *Nature*, 2002, **416**, 301.
- 14 J. R. Morber, Y. Ding, M. S. Haluska, Y. Li, J. P. Liu, Z. L. Wang and R. L. Snyder, *J. Phys. Chem. B*, 2006, **110**, 21672.
- 15 S. A. Wolf, D. D. Awschalom, R. A. Buhrman, J. M. Daughton, S. von Molnár, M. L. Roukes, A. Y. Chtchelkanova and D. M. Treger, *Science*, 2001, **294**, 1488.
- 16 R. S. Friedman, M. C. McAlpine, D. S. Ricketts, D. Ham and C. M. Lieber, *Nature*, 2005, **434**, 1085.
- 17 Z. M. Liao, Y. D. Li, J. Xu, J. M. Zhang, K. Xia and D. P. Yu, *Nano Lett.*, 2006, **6**, 1087.
- 18 X. Kou, X. Fan, R. K. Dumas, Q. Lu, Y. Zhang, H. Zhu, X. Zhang, K. Liu and J. Q. Xiao, *Adv. Mater.*, 2011, **23**, 1393.
- 19 Z. Z. Sun and J. Schliemann, *Phys. Rev. Lett.*, 2010, **104**, 037206.
- 20 X. H. Li, D. H. Zhang and J. S. Chen, *J. Am. Chem. Soc.*, 2006, **128**, 8382.
- 21 L. C. Palmer and S. I. Stupp, *Acc. Chem. Res.*, 2008, **41**, 1674.
- 22 C. Wang, Y. Hou, J. Kim and S. Sun, *Angew. Chem., Int. Ed.*, 2007, **46**, 6333.
- 23 M. Kwiat, S. Cohen, A. Pevzner and F. Patolsky, *Nano Today*, 2013, **8**, 677.
- 24 B. Mayers and Y. Xia, *J. Mater. Chem.*, 2002, **12**, 1875.
- 25 D. Ung, Y. Soumare, N. Chakroune, G. Viau, M. J. Vaulay, V. Richard and F. Fiévet, *Chem. Mater.*, 2007, **19**, 2084.
- 26 L. Bao, W. L. Low, J. Jiang and J. Y. Ying, *J. Mater. Chem.*, 2012, **22**, 7117.
- 27 A. K. Ganguli and T. Ahmad, *J. Nanosci. Nanotechnol.*, 2007, **7**, 2029.

- 28 T. Ahmad and A. K. Ganguli, Oxide Nanoparticles from Metal Oxalate Nanorods, in *Encyclopedia for Nanoscience and Nanotechnology*, American Scientific Publishers, 2011, vol. 20, p. 409.
- 29 Q. Wang and D. O'Hare, *Chem. Rev.*, 2012, **112**, 4124.
- 30 H. Bao, J. Yang, Y. Huang, Z. P. Xu, N. Hao, Z. Wu, G. Q. Lu and D. Zhao, *Nanoscale*, 2011, **3**, 4069.
- 31 S. He, Z. An, M. Wei, D. G. Evans and X. Duan, *Chem. Commun.*, 2013, **49**, 5912.
- 32 M. Shao, F. Ning, J. Zhao, M. Wei, D. G. Evans and X. Duan, *J. Am. Chem. Soc.*, 2011, **134**, 1071.
- 33 Z. P. Xu, G. S. Stevenson, C. Q. Lu, G. Q. Lu, P. F. Bartlett and P. P. Gray, *J. Am. Chem. Soc.*, 2005, **128**, 36.
- 34 X. Guo, F. Zhang, D. G. Evans and X. Duan, *Chem. Commun.*, 2010, **46**, 5197.
- 35 Y. Guo, H. Zhang, Y. Wang, Z. L. Liao, G. D. Li and J. S. Chen, *J. Phys. Chem. B*, 2005, **109**, 21602.
- 36 X. Yan, T. T. Tsotsis and M. Sahimi, *Microporous Mesoporous Mater.*, 2014, **190**, 267.
- 37 M. G. Kanatzidis, L. M. Tonge, T. J. Marks, H. O. Marcy and C. R. Kannewurf, *J. Am. Chem. Soc.*, 1987, **109**, 3797.
- 38 N. A. Frey, S. Peng, K. Cheng and S. Sun, *Chem. Soc. Rev.*, 2009, **38**, 2532.
- 39 H. Cao, R. Liang, D. Qian, J. Shao and M. Qu, *J. Phys. Chem. C*, 2011, **115**, 24688.
- 40 B. D. Cullity, *Introduction to magnetic materials*, Addison Wesley, Reading, MA, 1972, p. 410.